Realistic Microstructural RVE-Based Simulations of Stress-Strain Behavior of a Medium-Manganese Steels

J. M. Ran, X. Y. Hu, B. Zhu(✉), and Y. S. Zhang

State Key Laboratory of Materials Processing and Die and Mould Technology, Huazhong University of Science and Technology, Wuhan 430074, China
zhubin26@hust.edu.cn

Abstract. The mechanical properties of medium manganese steels with TRIP effect, which are typical of third generation automotive steels due to their high strength and plasticity are heavily dependent on their microstructure. Therefore, realistic microstructure based computational modeling of the mechanical behavior of medium manganese steels is built in the current research., and a user subroutine is developed to couple the martensitic phase transformation model. Virtual tensile process simulations are carried out using the representative volume element method to investigate the stress-strain partitioning and TRIP effects in the load-bearing process of medium-manganese steels. A comparison with experimental data is made to verify the accuracy of the method.

Keywords: Medium-manganese steels · Finite element method · Microstructure-based simulations

1 Introduction

The Mn content of medium manganese steel is about 3 ~ 12 percent. It has excellent performance. Such as high strength, good plasticity and other characteristics in line with the third generation of advanced high strength steel characteristics. Manganese steel as a potential candidate steel has been actively studied because of its good balance between material cost and mechanical properties. It makes use of TRIP effect plasticizing mechanism to redistribute stress and strain in different phases of steel during deformation. As a result, the local stress concentration is effectively alleviated, the strength and plasticity of medium manganese steel are enhanced, and the elongation of steel is improved. At present, the TRIP effect is mainly studied on TRIP steel composed of residual austenite, ferrite and bainite multiphase, but the medium manganese steel without deformation is a two-phase TRIP steel containing only ferrite and residual austenite [1]. And because

© The Author(s) 2023
Y. Zhang and M. Ma (Eds.): ICHSU 2022, AHMST 2, pp. 370–376, 2023.
https://doi.org/10.2991/978-94-6463-114-2_49

the concrete plastic instability behavior of medium manganese steel is different from that of traditional steel, there are few studies on the microstructure changes of medium manganese steel under the action of external forces, so the physical mechanism behind it is not clear. Therefore, RVE simulation of mechanical behavior of medium manganese steel based on real microstructure has profound significance.

In this study, the real microstructure of medium manganese steel obtained by SEM was used to establish a two-dimensional RVE finite element model. The criterion of martensitic transformation based on OC model [2] is introduced. On this basis, the ABAQUS phase change subroutine implemented by Fortran language is introduced. The microstructure evolution of medium manganese steel was successfully simulated by introducing the residual austenite phase change subroutine and without considering the phase change state. The effect of martensitic transformation on mechanical properties of medium manganese steel was studied.

2 Experimental

The composition of medium manganese steel used in this study is 0.06 wt% C, 6.0 wt% Mn and 0.95 wt% Al. The tensile test instrument is Shimadzu AG-100kN electronic universal testing machine. The tensile test was carried out in displacement controlled mode at room temperature. The tensile speed is 2 mm/min. After stretching, the engineering stress-strain curves and the flow stress-strain values of austenite, ferrite and martensite phases were obtained by nano indentation test for RVE simulation.

In this study, scanning electron microscope (SEM) was used to characterize the medium manganese steel samples before stretching. Thus, it is used to establish the microstructure of finite element simulation. The preparation of samples in the early stage of SEM detection can be roughly divided into three parts: insert, grinding and mechanical polishing. Immediately after mechanical polishing, rinse with alcohol and dry quickly with cold air. Then it can be used for SEM observation. The microstructure of the sample observed by SEM is shown in Fig. 1.

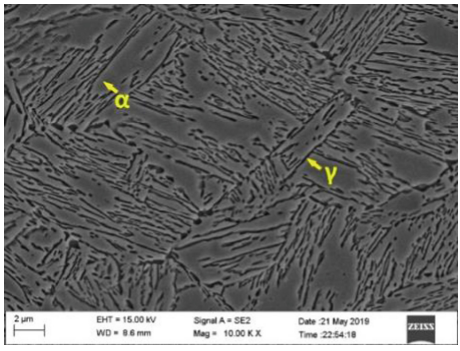

Fig. 1. Schematic diagram of the sample microstructure observed by SEM.

3 Finite Element Model and Boundary Conditions

3.1 Establishment of Finite Element Model

In this study, Python was used to segment SEM microstructure images to define the phase boundary between ferrite and residual austenite in materials. After obtaining the microstructure profile, the STP format file needed for RVE simulation was exported. The STP format files obtained after vectorization were imported into ABAQUS as sketches. Then a new shell with the same size as the microstructure diagram is built as the matrix of the material. Partition on the new shell using the imported sketch. The crust can be divided into ferrite and retained austenite. Then a two-dimensional plane model based on the actual microstructure of medium manganese steel as shown in Fig. 2 is established. Green represents residual austenite and white ferrite. It is then possible to set the parameters of the simulation so that the results can accurately reflect the mechanical properties of the experimental material.

3.2 Boundary Conditions

The establishment of appropriate boundary conditions is conducive to better simulation of uniaxial tensile test. RVE finite element simulation uses homogeneous boundary conditions. Boundary conditions are applied to the outer edge of the microstructure image, as shown in Fig. 3. The finite element simulation of uniaxial stress-strain characteristics is carried out under displacement control mode. The displacement is applied to the upper boundary along the Y-axis, which is also the loading direction of the tensile test. And the freedom of the upper boundary in the X direction is not constrained. All nodes along the left boundary are constrained in the X direction (not allowed to move), but are allowed to move unconstrained in the Y direction. All nodes along the lower edge are not allowed to move in the Y direction, but are free to move in the X direction. During tensile loading along the y direction, the nodes on the upper edge are also allowed to move along the X direction. In addition, the multi-node constraint is applied to all nodes on the right boundary requiring the same displacement in the X direction.

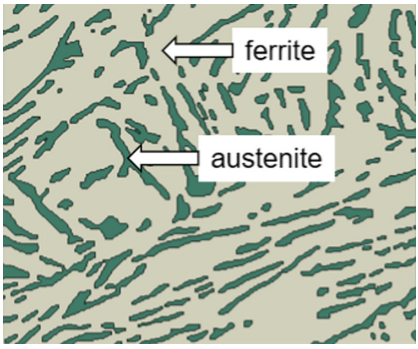

Fig. 2. Two-dimensional plane model of actual microstructure.

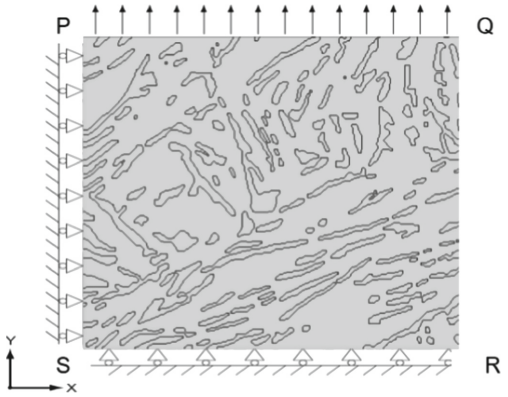

Fig. 3. Boundary conditions applied to microstructure.

4 Results and Discussion

4.1 Influence of Stress-Induced Martensitic Transformation on Stress-Strain Distribution of Medium Manganese Steel

Mises stress distribution was simulated from Fig. 4 under the strain condition of $\varepsilon = 14.69\%$. Austenite bears more stress than ferrite regardless of phase transition. It shows that ferrite is the soft phase and austenite is the hard phase under this strain. When the phase transformation process is not considered, the austenite stress distribution range is 1000–1250 MPa, and the ferrite stress distribution range is 860–980 MPa. After considering the transformation process, the stress distribution of austenite changes to 1050–2600 MPa, and the stress distribution range of ferrite hardly changes. It can be concluded that under the action of stress-induced martensitic transformation, the strain hardening ability is stronger than that of ferrite austenite. When the deformation of medium manganese steel reaches a certain threshold ($\pi_C = 15$ MPa), the residual austenite will be transformed into martensite. During the phase transformation, the volume fraction of martensite increases while that of retained austenite decreases. One of the main properties of martensite is its high strength and hardness. Therefore, the Mises stress was higher than that of the original austenite with improved mechanical properties. As a result, the overall strength of the material is increased and the plasticity is retained. Under the strain condition of $\varepsilon = 14.69\%$, the strain distribution of medium manganese steel can be seen from the true strain distribution in Fig. 5. That is, ferrite bears more strain than austenite regardless of whether martensitic transformation is considered. The strain distribution range of austenite under phase transformation is higher than that without martensitic transformation.

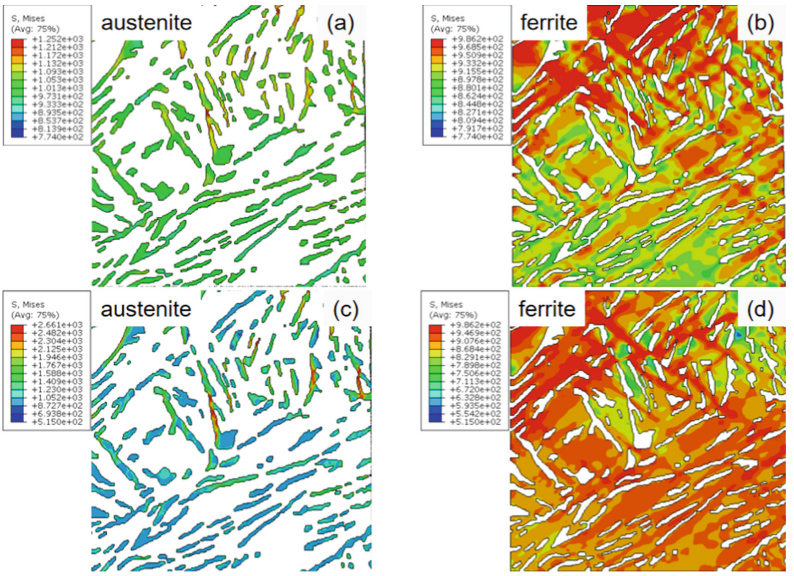

Fig. 4. Results of Mises stress distribution at $\varepsilon = 14.69\%$: (a) phase-free subroutine austenite; (b) Phase-free subroutine ferrite; (c) austenite with phase variant subroutine; (d) Austenite with phase variant subroutine.

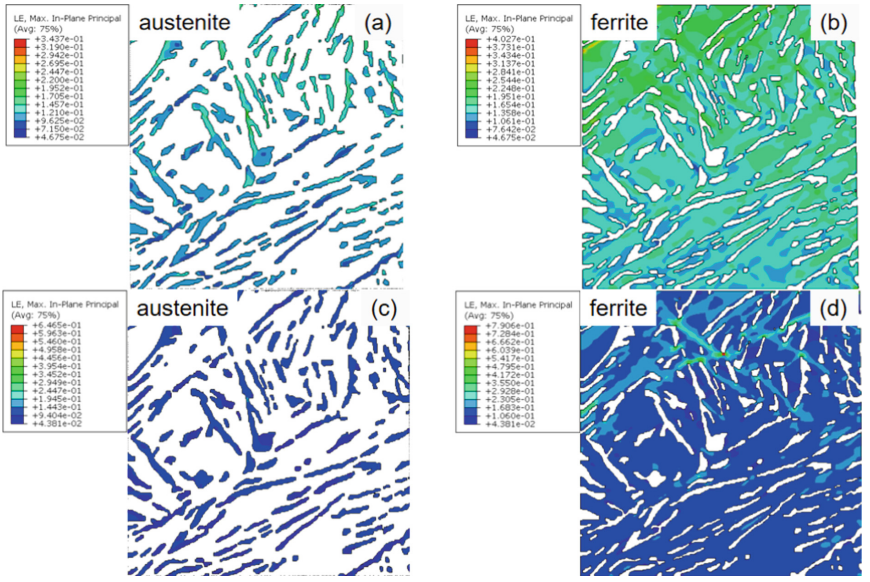

Fig. 5. Real strain distribution of simulation results when $\varepsilon = 14.69\%$: (a) phase-free subroutine austenite; (b) Phase-free subroutine ferrite; (c) austenite with phase variant subroutine; (d) Austenite with phase variant subroutine.

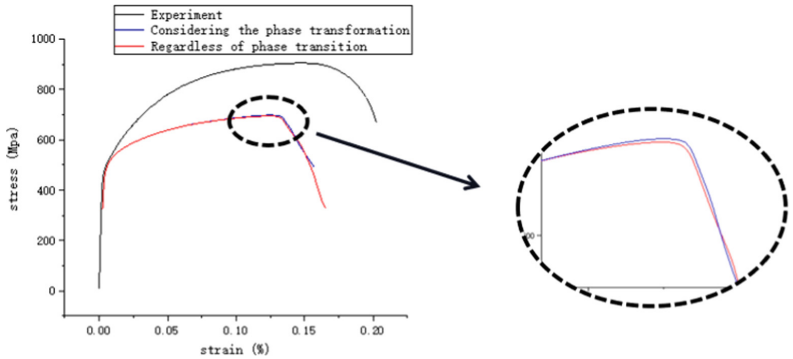

Fig. 6. Comparison of simulated and experimental stress-strain curves.

4.2 Comparative Analysis of Real Stress-Strain Curves in Experimental and Virtual Tensile Processes

Figure 6 shows the comparison of simulated and experimental stress-strain curves. It can be seen that the results of RVE simulation on the sample fit well with the real stress-strain curve obtained from the experiment, but the elastic deformation part of the simulation curve is longer than that of the experiment curve. And the yield stress of the three samples is much larger than the experimental results. After comprehensive analysis, it is likely that the stress - strain curves of each phase are inaccurate. Compared with the RVE simulation without considering phase transition, the fracture of the sample is delayed and its ultimate strength becomes higher when phase transition is considered. It shows that the ductility of medium manganese steel increases at this time, which verifies that the martensitic transformation in medium manganese steel will increase its elongation.

5 Conclusions

In this study, a two-dimensional plane RVE model established based on the real SEM microstructure was developed to simulate the microstructure evolution of medium manganese steel during virtual tension process, and martensitic transformation was coupled in the model. Based on this, a series of analyses are made. The main conclusions are as follows:

(1) Compared with the simulation results without phase change subroutine, the stress and strain distribution of residual austenite and ferrite changes with phase change considered. The distribution range of stress and strain under austenite becomes higher.
(2) The RVE simulation results of samples fit well with the real stress-strain curves obtained from experiments. Considering that the fracture of the sample is delayed and its ultimate strength becomes higher, it is verified that the medium martensitic transformation of medium manganese steel will increase its ductility and elongation.

References

1. Z. Cheng, X. Mao, W. R. Wang, X. C. Wei and Y. Y. Zhao, Study on constitutive relation of 0.1C-5Mn medium manganese steel considering TRIP effect, *Joumnal of Plasticity Engineering* **28**, 83 (2021).
2. G. B. Olson and C Morris, Kinetics of strain-induced martensitic nucleation, *Metallurgical Transactions A* **6**, 791 (1975).
3. D. K. Wang, X. Y. Cheng and S. Z. Wang, Research on retained austenite control and corrosion properties of mooring chain steel, *Shanghai Metal* **2**, 17 (2012).
4. J. Zhou, A. M. Gokhale, A. Gurumurthy and S. P. Bhat, Realistic microstructural RVE-based simulations of stress–strain behavior of a dual-phase steel having high martensite volume fraction, *Materials Science and Engineering: A* **630**, 107 (2015).
5. Y. Tomita and T Iwamoto, Constitutive modeling of trip steel and its application to the improvement of mechanical properties, *International Journal of Mechanical Sciences* **37**, 1295 (1995).

Open Access This chapter is licensed under the terms of the Creative Commons Attribution-NonCommercial 4.0 International License (http://creativecommons.org/licenses/by-nc/4.0/), which permits any noncommercial use, sharing, adaptation, distribution and reproduction in any medium or format, as long as you give appropriate credit to the original author(s) and the source, provide a link to the Creative Commons license and indicate if changes were made.

The images or other third party material in this chapter are included in the chapter's Creative Commons license, unless indicated otherwise in a credit line to the material. If material is not included in the chapter's Creative Commons license and your intended use is not permitted by statutory regulation or exceeds the permitted use, you will need to obtain permission directly from the copyright holder.